AppliedChem

MDPI

Article

One-Pot APTES Grafted Silica Synthesis and Modification with AgNPs

Gerardas Laurinavicius, Dovydas Karoblis and Vilius Poskus *

Faculty of Chemistry and Geosciences, Vilnius University, LT-08100 Vilnius, Lithuania; gerardas.laurinavicius@chgf.stud.vu.lt (G.L.); dovydas.karoblis@chgf.vu.lt (D.K.)
* Correspondence: vilius.poskus@chgf.vu.lt

Abstract

In today's chemistry, greener and more energy-efficient ways of making new materials are becoming increasingly important. In this work, two types of (3-aminopropyl) triethoxysilane-grafted silica were synthesized using a one-pot method with two different porogens: Pluronic P123 and cetyltrimethylammonium bromide, and then modified with silver nanoparticles. Both syntheses produced amorphous silica with crystalline silver. EDX and EDX elemental mapping confirmed that the modification with silver nanoparticles was successful, and an even distribution of silver on the silica surface with an average silver load of around 16% was determined. After silver nanoparticle modification, silica synthesized using cetyltrimethylammonium bromide as a porogen was mesoporous, whereas silica synthesis using Pluronic P123 as a porogen yielded a nonporous product. The synthesized silicas exhibited surface areas of 345 ± 2 and 8.80 ± 0.05 m^2/g for samples prepared using cetyltrimethylammonium bromide and Pluronic P123 as porogens, respectively, and both silicas were stable below 250 °C.

Keywords: silica; mesoporous materials; nonporous materials; silver nanoparticles

1. Introduction

Materials made from silica are widely used in various industrial and analytical chemistry fields. In industries, silica finds its place in building materials, desiccants, insulators, supports for catalysts and is used as an additive in the manufacture of several products [1]. In analytical chemistry, various types of organically modified silica are primarily used for biosensors, receptors, ion exchange coatings and different separations [2]. For example, aminated silica nanoparticles were used in the production of a biosensor for the detection of Aflatoxin B1, a highly toxic mycotoxin [3]. Ion-imprinted silica was utilized for U (VI) and Sc (I) removal from low-level radioactive effluents [4]. Additionally, silica is a key component in solid phase microextraction sorbents. Ionic liquid-coated silica in combination with gas chromatography was used for determination of seven organophosphorus insecticides in cucumber and grapefruit samples [5].

Unmodified silica sorbents are rarely used for analytical purposes. Typically, silica is modified with various organic functional groups or metal nanoparticles for the separation of specific compounds. Silicas, which are obtained after modification with organic groups, are referred to as organic–inorganic hybrid silica materials [6]. There are two main strategies used to prepare this type of compound: one-pot or post-synthesis grafting methods. In the one-pot method, already functionalized silica precursors are used to obtain the final product, whereas in the post-synthesis modification method, functional groups are introduced after

check for updates

Received: 7 September 2025
Revised: 3 October 2025
Accepted: 27 October 2025
Published: 3 November 2025

Citation: Laurinavicius, G.; Karoblis, D.; Poskus, V. One-Pot APTES Grafted Silica Synthesis and Modification with AgNPs. *AppliedChem* **2025**, *5*, 31. https://doi.org/10.3390/appliedchem5040031

the silica framework has been synthesized [7]. One-pot synthesis has many advantages compared to post-synthesis modification; it requires less time, uses low-toxicity materials, and, in vinyl-group-modified silica, the one-pot approach allows for obtaining higher functional group content, in comparison with post-synthesis modification [7,8].

One of the popular reagents used for silica functionalization is (3-aminopropyl) triethoxysilane (APTES). APTES-modified silica can be used on its own for the extraction and determination of various organic pollutants and trace elements using multiple analytical methods [9,10]. Another popular use of APTES-modified silica is its further modification with various biomolecules, such as antibodies or enzymes, for biosensors and diagnostic applications [11]. Sometimes the silica framework is modified via APTES groups to incorporate various metal nanoparticles. For example, gold nanoparticle-grafted silica was used for the separation and determination of steroid hormones [12]. Other metal nanoparticles, such as platinum and copper, can be attached to the silica surface [13,14].

One of the most popular metal nanoparticles to incorporate on the silica surface is silver nanoparticles (AgNPs). It is well known that silver has antibacterial properties; for example, silica films modified with AgNPs have shown good antibacterial properties against the E. coli bacterial strain [15]. AgNP-modified silica is also used in separation science. It was found that due to the interaction between AgNPs and double bonds, AgNP-loaded sorbents can separate various unsaturated compounds, such as polycyclic aromatic compounds and trans fatty acids [16,17]. When synthesizing silver nanoparticle-modified sorbents, as mentioned before, the sorbents are first modified with functional groups, usually APTES. When the silver ions are introduced, they form complexes with APTES amino groups, thus lowering the Ag^+ reduction potential from +0.799 to +0.373, and using a relatively weak reducing agent, such as formaldehyde, only the bonded silver ions are reduced to the AgNPs [16].

In this study, using a one-pot method, we synthesized two silicas modified with APTES with two different porogens—cetyltrimethylammonium bromide (CTAB) and Pluronic P123 (P123), and modified them with AgNPs. To our knowledge, similar types of sorbents are usually synthesized via a post-synthesis grafting method—our one-pot approach is less time-consuming and more environmentally friendly. We investigated how the use of different porogens and the incorporation of AgNPs influence the structural, morphological, textural, and thermal stability properties of the prepared silica, while also comparing our results with the same type of modified silicas, synthesized with post-synthesis methods, which are presented in the scientific literature.

2. Materials and Methods

2.1. Reagents

All chemicals used for synthesis and solutions were commercially available: tetramethyl orthosilicate (TMOS) (98%), Pluronic P123 (99.7%), and formaldehyde solution in water (37%) were purchased from Sigma Aldrich (St. Louis, MO, USA). APTES (98%) and acetic acid (99.7%) were obtained from Alfa Aesar (Ward Hill, MA, USA), and ethanol (96.3%) and CTAB (≥99%) were obtained from Vilniaus degtinė (Vilnius, Lithuania) and Carl Roth (Karlsruhe, Germany), respectively. Silver nitrate (99%) was obtained from Girochem (Teplička nad Váhom, Slovenia).

2.2. Characterization Methods

All samples were ground in an agate mortar prior to the characterization. X-ray diffraction (XRD) analysis was performed by a Miniflex II diffractometer (Rigaku, The Woodlands, TX, USA) using Cu Kα radiation (λ = 1.541838 Å) in a 2θ range from 10° to 80° with a step of 0.02° and a scanning speed of 5°/min. The crystallite size was

calculated using Scherrer's equation ($D = K\lambda/(\beta\cos\Theta)$), where K is the shape factor, λ is the X-ray wavelength, β is the full width at half maximum in radians, and Θ is the Bragg diffraction angle. To correctly determine the β for our samples, the β was measured for the corundum standard. Scanning electron microscopy (SEM) analysis was performed on a Hitachi SU-70 microscope. Elemental mapping for the powder samples was obtained by X-ray energy dispersive spectrometry (EDX) on Hitachi FlexSEM 1000 II (Hitachi, Tokyo, Japan) with an EDX detector. Each sample, before nitrogen adsorption–desorption, was degassed for 1.5 h at 120 °C under nitrogen flow using the FlowPrep 060 sample degas system (Micromeritics, Norcross, GA, USA). Nitrogen adsorption–desorption isotherms were measured using a TriStar II 3020 V1.03 instrument (Micrometrics, Norcross, GA, USA). Surface areas were calculated using the Brunauer–Emmett–Teller (BET) method and pore distribution (Barrett, Joyner, and Halenda) BJH method. Thermogravimetric analysis (TGA) was carried out using a Pyris 1 instrument (Perkin-Elmer Co., Norwalk, CT, USA) at a heating rate of 10 °C/min from 50 to 650 °C in nitrogen flow (20 mL/min). Powder Fourier-transform infrared spectroscopy (FT-IR) spectra of all compounds were recorded at ambient temperature in the range of 400 to 4000 cm^{-1} using a Bruker ALPHA-FTIR spectrometer (Bruker Optics, Billerica, MA, USA).

2.3. Synthesis of Uncoated Silicas

Silica with TMOS and APTES (1:1) was synthesized with P123 as a structure directing agent using the previous method [18] with some modifications. Firstly, 0.35 g of P123 was dissolved in 4 mL of 0.01 M acetic acid at room temperature (20 °C). After the complete dissolution of P123, the mixture was continuously stirred for 5 min in an ice bath (0 °C). Then, 491.5 µL APTES and 312.5 µL TMOS were added dropwise under vigorous stirring, and the reaction mixture was stirred for at least 3 min for a clear sol formation. The resultant solution was then transferred to a sealed container and kept at 60 °C for 3 days in the oven. To extract P123, synthesized silica was sonicated for 1 h in 30 mL of methanol in an ultrasonic bath. Then, if the silica was not going to be modified with AgNPs, the silica was dried at 40 °C for 5 days in the oven.

Silica, synthesized using CTAB as a structure directing agent and TMOS + APTES (1:1) as a silica source, was prepared by another method, with some modifications, described in the scientific literature [19]. Firstly, 236 µL APTES, 430 µL ethanol, 64 µL water, and 16 mg CTAB were mixed in a glass vial at room temperature (20 °C). After that, the mixture was placed in the ice bath (0 °C) for 5 min. Then the 149.2 µL TMOS was added dropwise, and the solution was thoroughly vortexed at room temperature for 30 s. The mixture was then reacted at 60 °C for 3 days in the oven and rinsed with ethanol 3 times for at least 12 h (solvent volume that was used each time—30 mL) to extract CTAB. Then, if the silica was not going to be modified with AgNPs, the silica was dried at 40 °C for 5 days in the oven.

2.4. Silica Modification with AgNPs

Silica's modification with AgNPs was performed using a method described in [16] with some modifications. After porogen extraction, the wet silicas were transferred into an amber glass vial with a 0.1 M ethanol solution of silver nitrate for 48 h at room temperature. Afterwards, the silicas were immersed in a 37% formaldehyde solution for 24 h. After that, the obtained silicas were washed 3 times with ethanol solution for at least 12 h each time and dried for 72 h at 40 °C in the oven.

3. Results

3.1. X-Ray Diffraction Analysis

A powder X-ray diffraction study was performed to investigate the influence of Ag coating on the structural properties of silica adsorbents, and the results are presented in Figure 1. As seen in Figure 1b and d, in unmodified silica cases, there is only one broad peak between 15° and 35° 2Θ values, which indicates the formation of amorphous silica. A similar XRD profile was observed for nano-silica prepared by the precipitation reaction of Na_2SiO_3 using H_2SO_4, where the formed SiO_2 gel was heated at 900 or 1000 °C [20]. It should be noted that the exact phase structure and cell parameters can be determined by performing small-angle XRD measurements [21], which are out of the scope of this study. When samples were coated with Ag (Figure 1a,c), the appearance of four distinct peaks, located at around 38°, 44°, 64°, and 77° 2Θ values, was observed. These XRD profiles of silicas, which were synthesized using two different porogens (P123 and CTAB) and coated with AgNPs, match the standard data of Ag (COD #96-901-3047). Similar results were observed for silica adsorbent loaded with AgNPs [22]. Silica, which was synthesized using P123 as a porogen and coated with AgNPs, displays broader diffraction peaks for the Ag phase, and the calculated crystallite size (silver crystals) for this sample is 9.6 ± 0.2 nm, while for silica that was synthesized using CTAB as a porogen, it is 16.4 ± 0.5 nm.

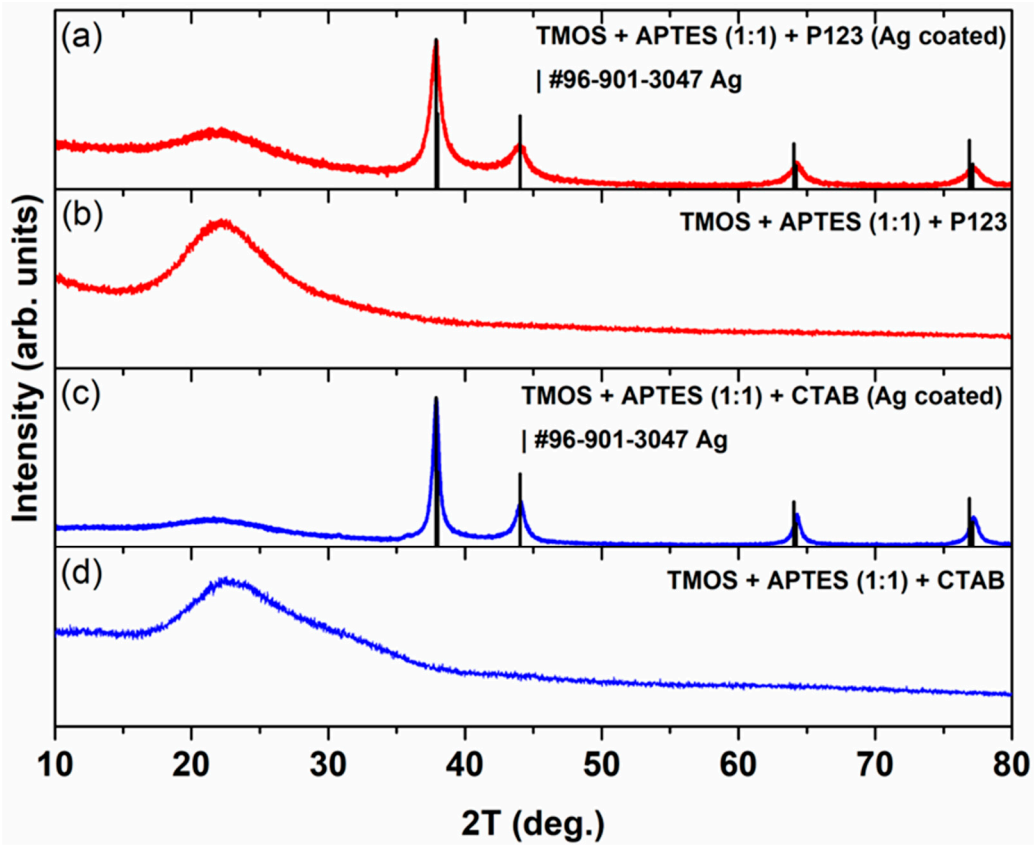

Figure 1. XRD pattern of silica, which was synthesized using CTAB as a porogen after (**a**) and before (**b**) its modification with AgNPs. XRD pattern of silica that was synthesized using P123 as a porogen after (**c**) and before (**d**) its modification with AgNPs.

3.2. Surface Morphology

In order to investigate how the different synthesis conditions and AgNP incorporation influenced the obtained silica surface morphology, scanning electron microscopy (SEM) was performed, and the results are presented in Figure 2. In our previous study [23], we observed that depending on the porogen used, the final silica products can have different

shapes and particle sizes. From Figure 2a,c, we can see that both silicas, synthesized using different porogens, have different particle structures. Silica that was synthesized using CTAB as a porogen (Figure 2a) has irregular particles, because glass-like monoliths are formed and their particle size cannot be adequately determined. When P123 is used as a porogen, silica has smooth and regular particles, which can be witnessed in Figure 2c. We can also see that after modification with AgNPs (Figure 2b,d), both silica particles' surfaces become rougher, indicating the presence of AgNPs on the surface. Similar morphological changes can also be seen in scientific literature; silica nanowire surface gets visibly rougher after its modification with silver and gold nanoparticles [24]. Moreover, silica nanoparticles, coated with AgNPs, can also be seen with a rough surface [25]. The overall particle structure of silica synthesized using CTAB as a porogen stays relatively the same after its modification with AgNPs (Figure 2a,b). In the P123 case (Figure 2c,d), after modification with AgNPs, silica particles become less spherical.

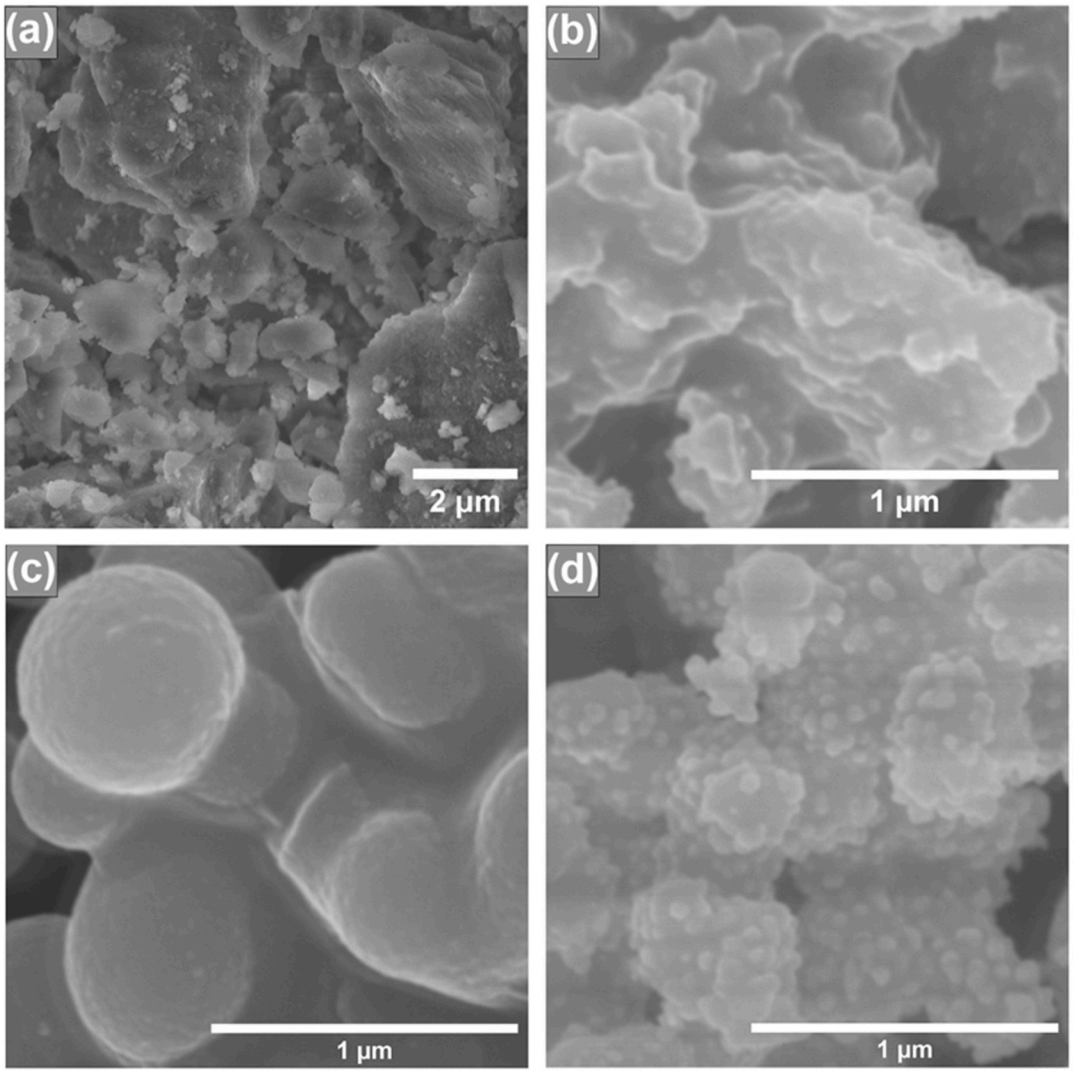

Figure 2. SEM images of synthesized silicas using CTAB as a structure directing agent before (**a**) and after (**b**) AgNP modification; SEM images of synthesized silicas using P123 as a structure directing agent before (**c**) and after (**d**) modification with AgNPs.

3.3. Elemental Analysis

To determine if the modification of silicas with AgNPs was successful, elemental analysis using X-ray energy dispersive spectrometry (EDX) was employed. It must be noted that the AgNP uncoated silicas are the intermediate compounds in this study; thus,

EDX data of those silicas are not presented. In Figure 3, we can see EDX images of synthesized silicas after modification with AgNPs. In all silicas, we can see that carbon, oxygen, aluminum, silicon, nitrogen, and silver peaks are visible; aluminum peaks arise from the aluminum sample holder, carbon from carbon tape, used to secure the samples on the aluminum holder. Oxygen and silicon peaks arise from silica itself. Silver peaks in both silicas confirm that the silica surface was successfully coated with AgNPs. Nitrogen peaks could arise from APTES groups that are immobilized on a silica surface. EDX measurements were also used to confirm APTES presence on mesoporous silica magnetite nanoparticles that were later used for the removal of Cr (VI) from aqueous solution [26]. Silver content, calculated against the silicon, in AgNP-coated silicas was 16.75 and 15.43 at% for silicas, synthesized using CTAB and P123 as a porogen, respectively.

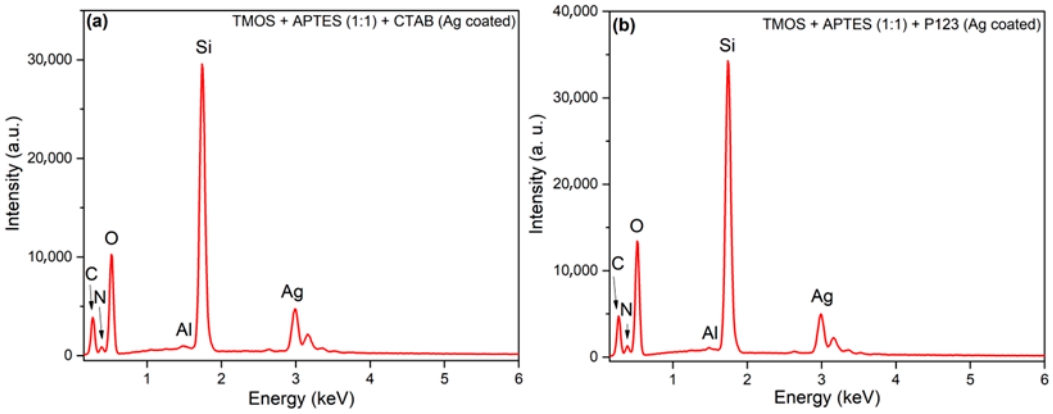

Figure 3. EDX images of synthesized silicas using CTAB as a structure directing agent (**a**) and using P123 as a structure directing agent (**b**) after modification with AgNPs.

EDX elemental mapping was also performed on silicas coated with AgNPs (Figure 4) to determine the distribution of elements. As shown in Figure 4, all elements—silicon (Si), oxygen (O), nitrogen (N), and silver (Ag)—in both silicas (synthesized by CTAB and P123) are homogeneously dispersed on the surface of silicas, and no Ag-rich regions were observed, indicating successful AgNP introduction.

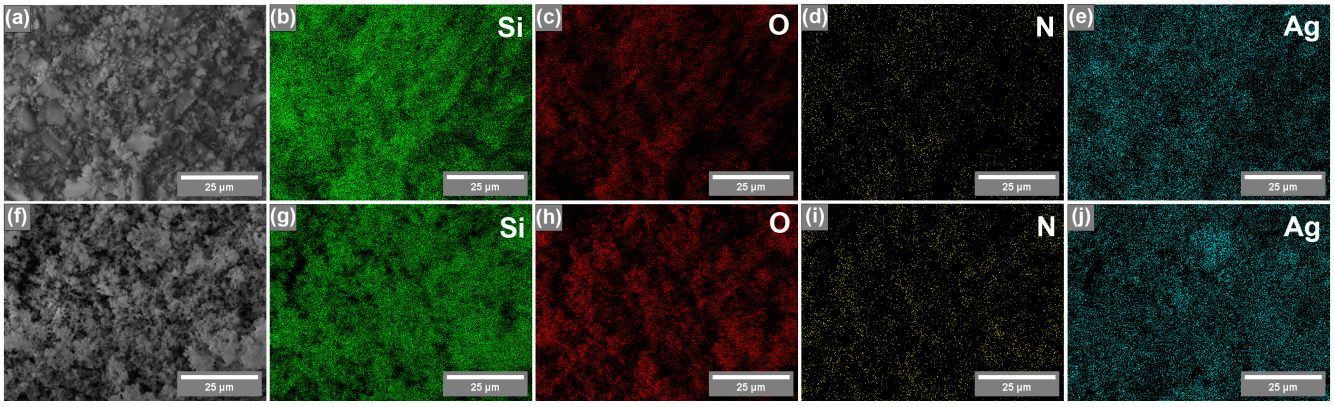

Figure 4. SEM image (**a**) and EDX elemental mapping of silica synthesized using CTAB as a porogen: Si (**b**), O (**c**), N (**d**), and Ag (**e**). SEM image (**f**) and EDX elemental mapping of silica synthesized using P123 as a porogen: Si (**g**), O (**h**), N (**i**), and Ag (**j**).

3.4. Textural Properties and Surface Area

To see if our synthesized silicas have the potential to be used as a base for sorbent synthesis, the nitrogen adsorption–desorption measurements were carried out, and the results are demonstrated in Figure 5. As depicted in Figure 5a, silica, which was synthesized

using CTAB as porogen and coated with AgNPs, has an IV-type hysteresis loop, associated with mesoporous materials [27]. In our previous study, similar results can be seen with silica, synthesized with the same reaction conditions but without AgNP modification [23]. These results indicate that modification with AgNPs does not have a significant impact on general porosity in this type of silica synthesis. These results correspond to the pore distribution data (Figure 5b); silica, modified with AgNPs, has mesopores. We can also see that modification with AgNPs increases the average pore size distribution compared to unmodified silica (Figure 5b).

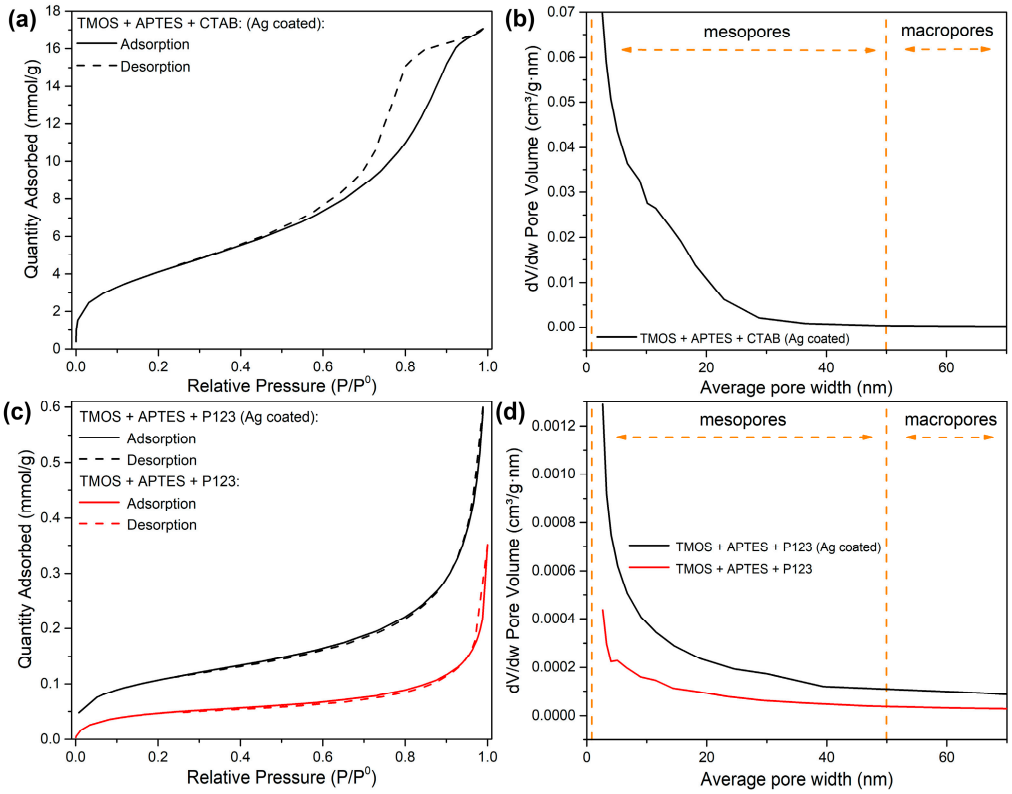

Figure 5. Nitrogen adsorption–desorption isotherms of synthesized silicas using CTAB as a structure directing agent after AgNP modification (**a**); pore volume distribution graph of synthesized silicas using CTAB as a structure directing agent after AgNP modification (**b**); nitrogen adsorption–desorption isotherms of synthesized silicas using P123 as a structure directing agent before (red line) and after (black line) modification with AgNPs (**c**); pore volume distribution graph of synthesized silicas using P123 as a structure directing agent before (red line) and after (black line) modification with AgNPs (**d**).

For silicas, synthesized using P123 as a porogen, we can indicate that both modified and unmodified silicas have type II isotherms (Figure 5c), which represent materials that are nonporous or macro porous (>50 nm pore size) [28]. These results are confirmed by pore distribution measurements (Figure 5d)—small pore volumes indicate that these silicas are nonporous. We can also see that after modification with AgNPs, pore volumes increase, especially in the small average pore size range, 2–10 nm (Figure 2d). This can be explained by the alteration of existing pore space when the AgNPs were deposited on a silica surface, for example, some pores or pore throats were split in a way that the smaller pores were formed after NP deposition. Similar effects were seen when the nanoparticles were injected into a porous sandy medium [29].

Pore distribution measurements suggest that the silica, synthesized via CTAB as a porogen and coated with AgNPs, has better application possibilities for sorbent synthesis than silica synthesized with P123 as a porogen and coated with AgNPs. Both nitrogen

adsorption–desorption isotherms and pore volume distribution graphs for uncoated silica, synthesized with CTAB as porogen, can be found in our previous work [23].

Surface areas were calculated using the Brunauer–Emmett–Teller (BET) method, and the results are presented in Table 1. As displayed in Table 1, unmodified silica that was synthesized using CTAB as a porogen has a much bigger surface area (175 ± 1 m^2/g) (the surface area was taken from [23]) in comparison with silica, synthesized using P123 as a porogen (3.95 ± 0.06 m^2/g). The same trend can be seen after AgNP modification with surface areas being 345 ± 2 and 8.80 ± 0.05 m^2/g, respectively. The AgNP introduction also leads to a double increase in surface area values, which confirms the successful silica modification. The increase in BET surface area can be explained by the increase in pore volume, as seen in Figure 5d for the silica synthesized using P123 as a porogen and for the silica synthesized using TMOS, APTES and CTAB after AgNP modification (Figure 5c) compared with the unmodified silica in our previous work, where the pore volume of the pores around the 2 nm mark are 0.05 $cm^3/g{\cdot}nm$ [23].

Table 1. Brunauer–Emmett–Teller (BET) surface areas of synthesized silicas.

Precursors Used in the Synthesis of Silicas	Surface Area, m^2/g
TMOS + APTES (1:1) + CTAB [1]	175 ± 1.1
TMOS + APTES (1:1) + CTAB (Ag coated)	345 ± 2
TMOS + APTES (1:1) + P123	3.95 ± 0.06
TMOS + APTES (1:1) + P123 (Ag Coated)	8.80 ± 0.05

[1] Surface area taken from article [23].

3.5. Thermostability Properties

Thermostability of both AgNP-coated silicas was evaluated using thermogravimetric analysis (TGA), and the results are illustrated in Figure 6. Because only the AgNP-coated silicas are the desirable product for future sorbent applications, the uncoated silicas' TGA results are not provided. Both silicas show a small weight loss at around 50–150 °C, which can be attributed to water loss. Another degradation step is observed from around 230 to 400 °C and can be attributed to weight loss from unwashed porogens (CTAB and P123) and pyrolysis of amino propyl groups from APTES [23]. These results correlate with EDX measurement and can explain the nitrogen presence in the synthesized silicas (Figures 3 and 4). Further weight loss from 400 to 600 °C can be attributed to the elimination of silanol groups [16]. These results demonstrate that better methods for removing porogens are needed, and amino propyl groups are immobilized on the silica surface. Also, the remaining unwashed P123 blocks the existing pores, which potentially explains the lack of porosity for this sample. In one study, authors suggest that P123 removal by calcination is necessary to obtain hexagonally ordered pores in mesoporous aluminosilicates [30].

3.6. Surface Functionalization

To examine the surface functionalization after the synthesis, the FT-IR spectroscopy was used, and the acquired results are depicted in Figure 7. Regardless of the synthesis method used, the FT-IR spectra of silica samples contain IR bands at around 1060 cm^{-1} and 810 cm^{-1}, which can be attributed to Si-O and Si-O-C stretching, respectively [28,31]. In both AgNP unmodified silicas (Figure 7, first and third lines), we can see bands around 1560 cm^{-1} that can be attributed to the N-H deformation peak from APTES [32]. N-H peaks in AgNP unmodified silica suggest that the APTES group's immobilization was successful. FTIR data of uncoated silica with CTAB were published in our previous work [23].

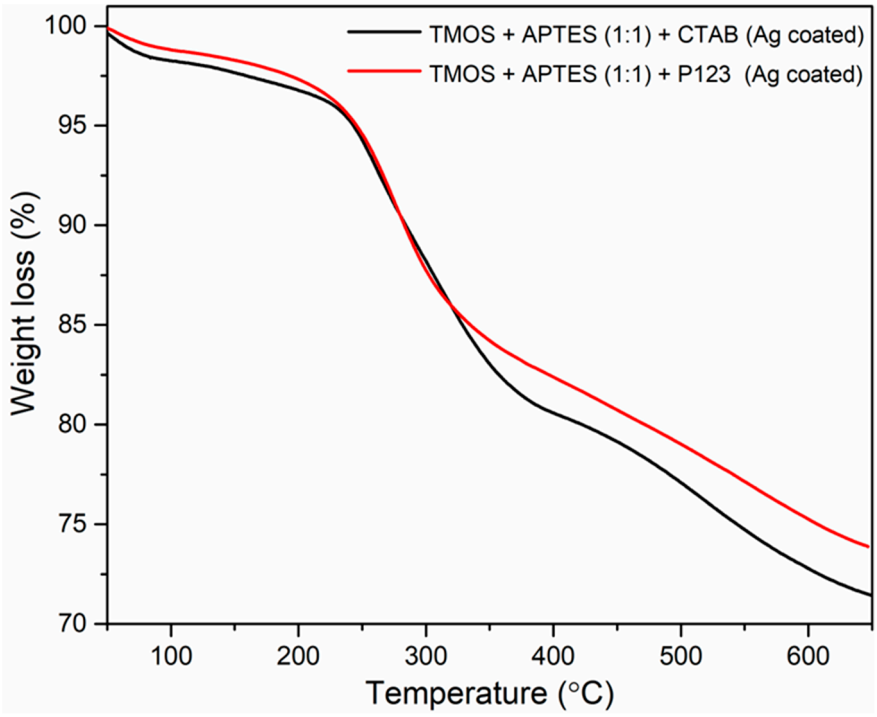

Figure 6. TGA measurements of synthesized silicas using CTAB as a structure directing agent (black line) and using P123 (red line) as a structure directing agent after modification with AgNPs.

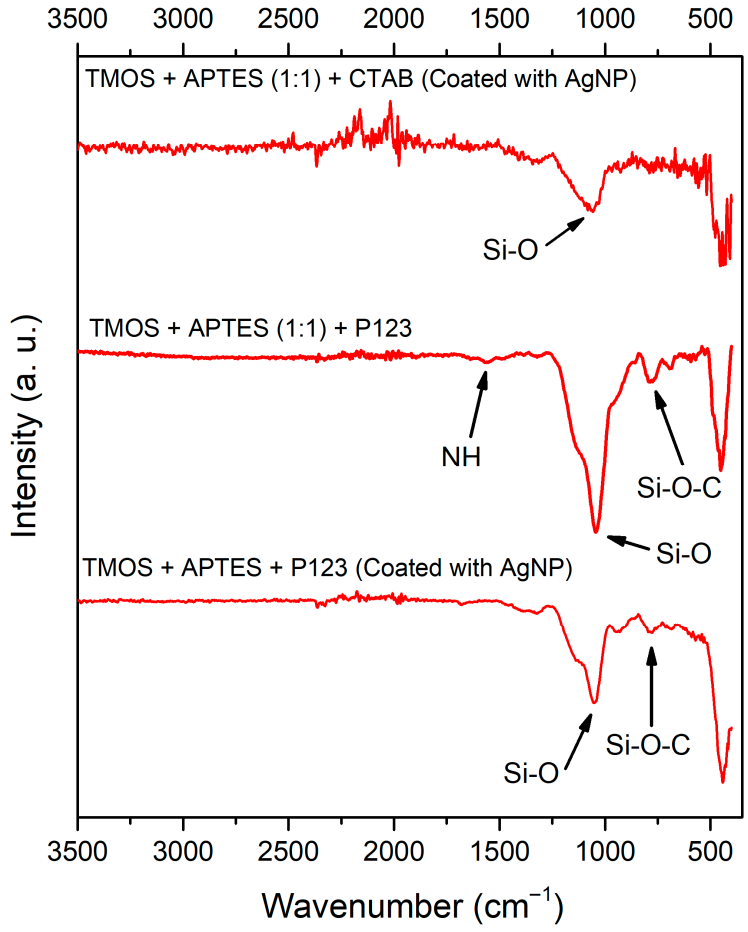

Figure 7. FT-IR spectra of synthesized silicas (from top to bottom): after AgNP modification, silica that was synthesized using P123 as a structure directing agent before and after modification with AgNPs.

4. Discussion

When comparing the structural properties of AgNP-coated silica obtained via one-pot with post-synthesis grafting methods, we can observe similar XRD profiles in both cases: a broad peak, which can be attributed to the amorphous silica, and sharp peaks, belonging to the Ag crystalline phase in the cases of both porogens (P123 and CTAB) [16,33]. We can conclude that in both porogen cases, the crystal structure stays relatively the same when comparing the one-pot and post-synthesis grafting methods.

Materials, which are used as sorbents, should have good porosity, ideally in the mesopore range, and high surface area. Mesoporous materials, according to the nomenclature by the International Union of Pure and Applied Chemistry (IUPAC), are materials with pore sizes ranging from 2 to 50 nm [27]. Mesoporous materials, synthesized by varying various porogens and reaction conditions, can be synthesized with high surface areas (>1000 m^2/g) but also with large pore volumes (1 cm^3/g) and narrow pore distribution [34]. Other mesoporous materials' advantages in separation science are the size-selective adsorption of small molecules (particularly excluding larger ones), thermal stability, chemical stability, compositional controllability, and possibility of post-synthesis modification by introducing various functional groups for different separation properties [35]. Silica synthesized using P123 as a porogen and modified with AgNPs is not an ideal choice—the low surface area and lack of mesopores limit its application in separation science. In contrast, silica synthesized using CTAB as a porogen and modified with AgNPs potentially can be used for future sorbent development. For example, in a related study where silica was used with TMOS as a silica source and urea as a catalyst, nitrogen adsorption–desorption revealed the formation of ordered mesopores with narrow pore size and a surface area of 393 m^2/g (before the modification with APTES and AgNPs) [16]. After modification with AgNPs, the silica was successfully applied for the separation of aromatic hydrocarbons [16]. While the procedure of incorporating AgNPs in this study was nothing new—it was successfully used in previous works—it is important to notice that usually the incorporation of AgNPs is performed on a post-grafting synthesis, where APTES is not used as a silica source. In this case, APTES functional groups are directly incorporated into the silica framework and have an impact on initial pore formation, resulting in a shift towards micro pores, while still producing the pores in the mesopore range. For example, in the post-synthesis grafting methods, the pores are usually in the narrow 5 to 10 nm range [16,36]. When comparing our results with previously reported synthesis, we can see that this change in the starting reaction mixture, while broadening pore size distribution, still produces the pores in the 5–10 nm range, typical for previously mentioned post-grafting methods. The impact of this change in pore size distribution, while being an important topic for developing future sorbents, is out of the scope of this investigation.

Another important property of sorbents, especially in gas chromatography analysis when the sorbent is inserted directly into the injection port, is thermal stability. Typically, desorption temperature is set between 100 and 300 °C, depending on the volatility and thermal stability of analytes of interest [18,37–39]. As mentioned earlier, AgNP-modified sorbents can be used for the extraction of unsaturated compounds. For instance, literature reports show that naphthalene and anthracene were successfully extracted and desorbed from the sample headspace using silica sorbent, with the injection port temperature (where desorption happens) set at 200 °C [18]. In our case, both silicas could be used for this purpose, as both silicas start to decompose around 230 °C.

The environmental and time aspects of this study should also be noted. In this type of silica synthesis, typically, the post-synthesis grafting method is used with a separate stage for aminopropyl group grafting, where the silica is treated with the APTES solution in toluene at 80 °C [16]. Eliminating this stage from the synthesis reduces the need for toxic

solvents (toluene) and reduces the energy consumption because heating at 80 °C for 24 h is not needed in this situation. Moreover, the additional washing step after aminopropyl modification is not needed, further reducing the synthesis time and economic cost of the whole process.

5. Conclusions

In this work, two silicas, coated with AgNPs, were successfully synthesized using TMOS and APTES as silica sources, with CTAB or P123 as a porogen. Both synthesized silicas exhibited an amorphous silica phase and crystalline silver nanoparticles with uniform element distribution on the surface. Both silicas were thermally stable up to 250 °C. Silica synthesized using CTBA and modified with AgNPs displayed mesopores with a BET surface area of 345 $\pm$ 2 m^2/g, whereas silica synthesized using P123 as a porogen and coated with AgNPs was nonporous, with a BET surface area of 8.80 $\pm$ 0.05 m^2/g. Comparison with literature data indicates that silica synthesized using CTAB and coated with AgNPs has potential for future sorbent development, as its thermal stability, surface area, and porosity are similar to those of previously reported sorbents. These results show that it is possible to synthesize porous silica, coated with AgNPs, with a synthesis that requires less time and toxic chemicals, compared to more traditional synthesis methods, while at the same time achieving comparable specifications, like surface area, porosity, and thermal stability.

Author Contributions: Conceptualization, G.L. and D.K.; methodology, G.L.; investigation, G.L. and D.K.; data curation, G.L.; writing—original draft preparation, G.L. and D.K.; writing—review and editing, G.L., D.K. and V.P.; visualization, G.L.; supervision, V.P.; All authors have read and agreed to the published version of the manuscript.

Funding: This research received no external funding.

Institutional Review Board Statement: Not applicable.

Informed Consent Statement: Not applicable.

Data Availability Statement: Dataset available on request from the authors.

Acknowledgments: The authors thankfully acknowledge Eglė Ežerskytė for providing the nitrogen adsorption–desorption measurements and Giedrė Gaidamavičienė for providing TGA measurements.

Conflicts of Interest: The authors declare no conflicts of interest.

Abbreviations

The following abbreviations are used in this manuscript:

AgNPs	Silver nanoparticles
APTES	3-aminopropyl) triethoxysilane
TMOS	Tetramethyl orthosilicate
P123	Pluronic P123
CTAB	Cetyltrimethylammonium bromide
XRD	X-ray diffraction
EDX	X-ray energy dispersive spectrometry
TGA	Thermogravimetric analysis
FTIR	Fourier Transform Infrared Spectroscopy

References

1. Flörke, O.W.; Graetsch, H.A.; Brunk, F.; Benda, L.; Paschen, S.; Bergna, H.E.; Roberts, W.O.; Welsh, W.A.; Libanati, C.; Ettlinger, M.; et al. *Ullmann's Encyclopedia of Industrial Chemistry*; Wiley: Hoboken, NJ, USA, 2008.

2. Collinson, M.M. Recent Trends in Analytical Applications of Organically Modified Silicate Materials. *TrAC Trends Anal. Chem.* **2002**, *21*, 31–39. [CrossRef]
3. Wu, Z.; Sun, D.W.; Pu, H.; Wei, Q. A Dual Signal-on Biosensor Based on Dual-Gated Locked Mesoporous Silica Nanoparticles for the Detection of Aflatoxin B1. *Talanta* **2023**, *253*, 124027. [CrossRef]
4. Zhou, L.; Xu, M.; Yin, J.; Shui, R.; Yang, S.; Hua, D. Dual Ion-Imprinted Mesoporous Silica for Selective Adsorption of U(VI) and Cs(I) through Multiple Interactions. *ACS Appl. Mater. Interfaces* **2021**, *13*, 6322–6330. [CrossRef] [PubMed]
5. Delińska, K.; Yavir, K.; Kloskowski, A. Head-Space SPME for the Analysis of Organophosphorus Insecticides by Novel Silica IL-Based Fibers in Real Samples. *Molecules* **2022**, *27*, 4688. [CrossRef]
6. Wahab, M.A.; Guo, W.; Cho, W.-J.; Ha, C.-S. Synthesis and Characterization of Novel Amorphous Hybrid Silica Materials. *J. Sol-Gel Sci. Technol.* **2003**, *27*, 333–341. [CrossRef]
7. Zajickova, Z. Review of Recent Advances in Development and Applications of Organic-Silica Hybrid Monoliths. *J. Sep. Sci.* **2023**, *46*, 2300396. [CrossRef]
8. El-Debs, R.; Cadoux, F.; Bois, L.; Bonhommé, A.; Randon, J.; Dugas, V.; Demesmay, C. Synthesis and Surface Reactivity of Vinylized Macroporous Silica Monoliths: One-Pot Hybrid versus Postsynthesis Grafting Strategies. *Langmuir* **2015**, *31*, 11649–11658. [CrossRef]
9. Otalvaro, J.O.; Avena, M.; Brigante, M. Adsorption of Organic Pollutants by Amine Functionalized Mesoporous Silica in Aqueous Solution. Effects of PH, Ionic Strength and Some Consequences of APTES Stability. *J. Environ. Chem. Eng.* **2019**, *7*, 103325. [CrossRef]
10. Zhang, L.; Chen, B.; Peng, H.; He, M.; Hu, B. Aminopropyltriethoxysilane-Silica Hybrid Monolithic Capillary Microextraction Combined with Inductively Coupled Plasma Mass Spectrometry for the Determination of Trace Elements in Biological Samples. *J. Sep. Sci.* **2011**, *34*, 2247–2254. [CrossRef]
11. Vashist, S.K.; Lam, E.; Hrapovic, S.; Male, K.B.; Luong, J.H.T. Immobilization of Antibodies and Enzymes on 3-Aminopropyltriethoxysilane-Functionalized Bioanalytical Platforms for Biosensors and Diagnostics. *Chem. Rev.* **2014**, *114*, 11083–11130. [CrossRef]
12. Amoli-Diva, M.; Pourghazi, K. Gold Nanoparticles Grafted Modified Silica Gel as a New Stationary Phase for Separation and Determination of Steroid Hormones by Thin Layer Chromatography. *J. Food Drug. Anal.* **2015**, *23*, 279–286. [CrossRef]
13. Kobayashi, Y.; Sakuraba, T. Silica-Coating of Metallic Copper Nanoparticles in Aqueous Solution. *Colloids Surf. A Physicochem. Eng. Asp.* **2008**, *317*, 756–759. [CrossRef]
14. Dag, Ö.; Samarskaya, O.; Coombs, N.; Ozin, G.A. The Synthesis of Mesostructured Silica Films and Monoliths Functionalised by Noble Metal Nanoparticles. *J. Mater. Chem.* **2003**, *13*, 328–334. [CrossRef]
15. Pal, S.; Nisi, R.; Licciulli, A. Antibacterial Activity of In Situ Generated Silver Nanoparticles in Hybrid Silica Films. *Photochem* **2022**, *2*, 479–488. [CrossRef]
16. Zhu, Y.; Morisato, K.; Li, W.; Kanamori, K.; Nakanishi, K. Synthesis of Silver Nanoparticles Confined in Hierarchically Porous Monolithic Silica: A New Function in Aromatic Hydrocarbon Separations. *ACS Appl. Mater. Interfaces* **2013**, *5*, 2118–2125. [CrossRef]
17. Poškus, V.; Vičkačkaitė, V. Silver-coated Monolithic Silica Column for Separation of Trans Fatty Acids. *Sep. Sci. Plus* **2018**, *1*, 738–745. [CrossRef]
18. Laurinavičius, G.; Poškus, V. Synthesis and Investigation of Silver-Coated Monolithic Solid Phase Microextraction Silica Sorbent. *Chemija* **2023**, *34*, 41–47. [CrossRef]
19. Yan, L.; Zhang, Q.; Zhang, J.; Zhang, L.; Li, T.; Feng, Y.; Zhang, L.; Zhang, W.; Zhang, Y. Hybrid Organic-Inorganic Monolithic Stationary Phase for Acidic Compounds Separation by Capillary Electrochromatography. *J. Chromatogr. A* **2004**, *1046*, 255–261. [CrossRef]
20. EL-Rafei, A.M. Preparation and Characterization of Mesoporous Amorphous Nano-Silica and Nano-Cristobalite for Value Enhancement of Low-Cost Egyptian Waste Materials. *Ceram. Int.* **2022**, *48*, 32185–32195. [CrossRef]
21. Chandrasekar, G.; You, K.S.; Ahn, J.W.; Ahn, W.S. Synthesis of Hexagonal and Cubic Mesoporous Silica Using Power Plant Bottom Ash. *Microporous Mesoporous Mater.* **2008**, *111*, 455–462. [CrossRef]
22. Thamilselvi, V.; Radha, K.V. Silver Nanoparticle Loaded Silica Adsorbent for Wastewater Treatment. *Korean J. Chem. Eng.* **2017**, *34*, 1801–1812. [CrossRef]
23. Laurinavičius, G.; Poškus, V. Mesoporous Silica Synthesis: Different Precursors, Catalysts and Structure Directing Agents. *Silicon* **2025**, *17*, 2381–2391. [CrossRef]
24. Convertino, A.; Cuscunà, M.; Martelli, F.; Manera, M.G.; Rella, R. Silica Nanowires Decorated with Metal Nanoparticles for Refractive Index Sensors: Three-Dimensional Metal Arrays and Light Trapping at Plasmonic Resonances. *J. Phys. Chem. C* **2014**, *118*, 685–690. [CrossRef]

25. Park, S.H.; Ko, Y.S.; Park, S.J.; Lee, J.S.; Cho, J.; Baek, K.Y.; Kim, I.T.; Woo, K.; Lee, J.H. Immobilization of Silver Nanoparticle-Decorated Silica Particles on Polyamide Thin Film Composite Membranes for Antibacterial Properties. *J. Memb. Sci.* **2016**, *499*, 80–91. [CrossRef]
26. Hozhabr Araghi, S.; Entezari, M.H.; Chamsaz, M. Modification of Mesoporous Silica Magnetite Nanoparticles by 3-Aminopropyltriethoxysilane for the Removal of Cr(VI) from Aqueous Solution. *Microporous Mesoporous Mater.* **2015**, *218*, 101–111. [CrossRef]
27. Thommes, M.; Kaneko, K.; Neimark, A.V.; Olivier, J.P.; Rodriguez-Reinoso, F.; Rouquerol, J.; Sing, K.S.W. Physisorption of Gases, with Special Reference to the Evaluation of Surface Area and Pore Size Distribution (IUPAC Technical Report). *Pure Appl. Chem.* **2015**, *87*, 1051–1069. [CrossRef]
28. Gutierrez-Climente, R.; Gomez-Caballero, A.; Guerreiro, A.; Garcia-Mutio, D.; Unceta, N.; Goicolea, M.A.; Barrio, R.J. Molecularly Imprinted Nanoparticles Grafted to Porous Silica as Chiral Selectors in Liquid Chromatography. *J. Chromatogr. A* **2017**, *1508*, 53–64. [CrossRef]
29. Fopa, R.D.; Bianco, C.; Archilha, N.L.; Moreira, A.C.; Pak, T. A Pore-Scale Investigation of the Effect of Nanoparticle Injection on Properties of Sandy Porous Media. *J. Contam. Hydrol.* **2023**, *253*, 104126. [CrossRef] [PubMed]
30. Jin, J.; Cao, L.; Su, G.; Xu, C.; Zhang, Z.; Gao, X.; Liu, H.; Liu, H. A Facile Strategy to Recycle Template P123 from Mesoporous Aluminosilicates by Ultrasonic Extraction. *Ultrason. Sonochem.* **2014**, *21*, 1688–1695. [CrossRef]
31. Criado, M.; Sobrados, I.; Sanz, J. Polymerization of Hybrid Organic-Inorganic Materials from Several Silicon Compounds Followed by TGA/DTA, FTIR and NMR Techniques. *Prog. Org. Coat* **2014**, *77*, 880–891. [CrossRef]
32. Anbia, M.; Lashgari, M. Synthesis of Amino-Modified Ordered Mesoporous Silica as a New Nano Sorbent for the Removal of Chlorophenols from Aqueous Media. *Chem. Eng. J.* **2009**, *150*, 555–560. [CrossRef]
33. Abduraimova, A.; Molkenova, A.; Duisembekova, A.; Mulikova, T.; Kanayeva, D.; Atabaev, T.S. Cetyltrimethylammonium Bromide (Ctab)-Loaded Sio2–Ag Mesoporous Nanocomposite as an Efficient Antibacterial Agent. *Nanomaterials* **2021**, *11*, 477. [CrossRef]
34. Alothman, Z.A. A Review: Fundamental Aspects of Silicate Mesoporous Materials. *Materials* **2012**, *5*, 2874–2902. [CrossRef]
35. Zhao, L.; Qin, H.; Wu, R.; Zou, H. Recent Advances of Mesoporous Materials in Sample Preparation. *J. Chromatogr. A* **2012**, *1228*, 193–204. [CrossRef]
36. Yu, H.; Zhu, Y.; Yang, H.; Nakanishi, K.; Kanamori, K.; Guo, X. Facile Preparation of Silver Nanoparticles Homogeneously Immobilized in Hierarchically Monolithic Silica Using Ethylene Glycol as Reductant. *Dalton Trans.* **2014**, *43*, 12648–12656. [CrossRef]
37. Gaffke, A.M.; Alborn, H.T. Desorption Temperature, Solid-Phase Microextraction (SPME), and Natural Product Analyses, How Low Can We Go? *J. Chem. Ecol.* **2021**, *47*, 134–138. [CrossRef]
38. Hook, G.L.; Kimm, G.L.; Hall, T.; Smith, P.A. Solid-Phase Microextraction (SPME) for Rapid Field Sampling and Analysis by Gas Chromatography-Mass Spectrometry (GC-MS). *TrAC Trends Anal. Chem.* **2002**, *21*, 534–543. [CrossRef]
39. Bryant, R.J.; McClung, A.M. Volatile Profiles of Aromatic and Non-Aromatic Rice Cultivars Using SPME/GC-MS. *Food Chem.* **2011**, *124*, 501–513. [CrossRef]